Smart Structures and Systems, *Vol. 27, No. 4 (2021) 847-860*
DOI: https://doi.org/10.12989/sss.2021.27.4.847

A new quasi-3D theory for the study of the bending of thick FGM's plates on elastic foundation

Abdelghani Belarouci* and Abdelkader Fekrar

Faculty of Technology, Civil Engineering and Public Works Department, University of Sidi Bel Abbes, BP 89 cite Ben M'hidi 22000 Sidi Bel-Abbes, Algeria

(*Received April 2, 2020, Revised December 16, 2020, Accepted January 27, 2021*)

Abstract. In this work, a new theory quasi-3D shear deformation is presented to analyze the bending of thick FGM (functionally graded materials) plates resting on Pasternak elastic foundations, whose number of variables is limited to five. The mathematical model used presents a new range of displacement based on indeterminate integral variables where the stretching of thickness is taken into account according to the power laws P-FGM, E-FGM and S-FGM. The compositions and volume fractions of the constituents in the FGM are supposed to change through the thickness. The principle of virtual work, as well as the Naiver method, is used in this study to solve the governing equations of motion to study these types of plates. The equilibrium equations according to the FG plate resting on Pasternak foundations are presented. The results obtained are compared to those determined by the other authors**.** It was observed from the comparative studies that quasi-3D theories that take into account thickness stretching effects can predict bending behavior more accurately than other theories.

Keywords: FGM plates; bending thick plates; Quasi 3-D theory; the stretching effect; Pasternak

1. Introduction

Functional Gradation Materials are a class of composites that exhibit a continuous variation in material properties from one surface to another. A typical FGM is made from a blend of two material phases, for example, a ceramic and a metal, with mechanical and thermal properties that vary continuously through the thickness of the material. Faced with problems related to the durability of conventional materials such as degradation caused by aging, corrosion, exposure to high temperatures, and other degradation phenomena, FGM remains the optimal material in the environment where it is exposed. The FGM plates that are the subject of this study are made from a mixture of metal and ceramic. Currently, these FGM materials are widely used throughout aerospace, automotive, civil and mechanical engineering structures and their material properties can be adapted to different applications, and working environments. Many kinds of research and studies on the FGM structures (Bouazza *et al*. 2015, Benahmed *et al*. 2019). Plates resting on elastic foundations are among the preoccupations of researchers to model various engineering problems over the last decades.

In the last years, laminates presented a problem specific to composite materials produced by lamination: It is the interlaminar rupture, known under the technical name of "Delamination". By the finite element method, Hirwani *et al*. (2018a) studied the deflection responses of shallow double-curved hull panels damaged under combined thermomechanical loading where they were able to obtain, with some new solved examples, the deflection responses under the influence of thermomechanical loading. the transient behavior of a laminated composite plate and an internally damaged shell structure under the influence of different types of mechanical loads and stress conditions have been numerically analyzed by Hirwani *et al*. (2017), where internal delamination is modeled using two substratified approaches including the condition of intermittent continuity to obtain the necessary solutions. Nonlinear flexural analysis of laminated composite flat panel under hygro-thermo-mechanical loading has been analyzed by Kar *et al*. (2015). Curved panel structures using higher-order theory have been analyzed by Katariya *et al*. (2019), Hirwani and Panda (2019). Hygrothermal effects on the postbuckling response of composite beams have been analyzed by Bouazza *et al*. (2014a). Abdelmalek *et al*. (2017) studies the hygrothermal effects on the free vibration behavior of composite plate using nth-order shear deformation theory. The novel generation of composite materials introduced in nanotechnology, which are (FG-CNT) functionally graded distributions of carbon nanotube in the thickness direction, has provided solutions to many technical problems (Guessas *et al*. 2018, Boulal *et al*. 2020, Tayeb *et al*. 2020, Zerrouki *et al*. 2020, Gafour *et al*. 2020, Bensattalah *et al*. 2018a, b, 2019a, Hamidi *et al*. 2018, Dihaj *et al*. 2018, Belmahi *et al*. 2018, Belmahi *et al*. 2019). Due to the importance of CNT in nanocomposites, several theoretical approaches have been developed to study their mechanical behavior (Bouazza *et al*. 2014b, Bensattalah *et al*. 2019b, c).

The attempt to produce Functional Gradient Materials arose from mixing two materials in such a way that both

*Corresponding author,
E-mail: abelarouci@yahoo.fr

ISSN: 1738-1584 (Print), 1738-1991 (Online)

materials retain their physical, mechanical and thermal properties most efficiently. The resulting FGM material shows a gradation across the depth of the structure, from a typically metallic material such as steel or aluminum on one side of the depth, to another material such as ceramic on the other side. Therefore, Functional or Functionally Graduated Gradient Material is a new range of composite materials having a gradual and continuous variation of the volume fractions of each of the constituents (in general, metal and ceramic) through the thickness, inducing changes, as a consequence of the overall thermo-mechanical properties of the structural element that it constitutes. The non-linear bending behavior of a functionally graded curved panel (cylindrical, hyperbolic and elliptical) under combined thermomechanical loading is studied by Kar and Panda (2016). In this study, two temperature fields (uniform and linear) over the thickness of the shell panel are considered. The panel model is mathematically developed using higher-order shear strain mid-plane kinematics with Green - Lagrange type nonlinear deformations. Kar and Panda (2015) have also numerically studied the large amplitude bending behavior of a functionally graded double-curved hull panel under thermomechanical loading.

The power law function (P-FGM) and the exponential function (E-FGM) are commonly used to describe variations in the material properties of FGMs. Therefore, other authors proposed a refined higher order shear and normal deformation theory for E-, P-, and S-FGM plates on Pasternak elastic foundation (Lee *et al*. 2015). The bending and vibration behavior of FG plates has been studied by many researchers over the last ten years. Neves *et al*. (2012) presented the equations of a sinusoidal quasi-3D shear deformation theory for FG plates. It addresses the free vibration and bending analysis and accounts for through-the-thickness deformations. To analyze bending, analytical solutions are obtained for simply supported plates using the equations of motion according to the principle of minimum total potential energy. It is accepted that the elastic medium is demonstrated as a Winkler-Pasternak elastic foundation. Zenkour (2009) studied several cases to demonstrate the numerical results concerning the bending response of rectangular plates resting on Winkler elastic foundations.

Panda and Singh (2013) studied the thermal post buckling behavior of laminated composite spherical shell panels. Shokravi (2017) presented the vibration analysis of silica nanoparticles-reinforced concrete beams considering agglomeration effects. Wu and Liu (2014) analyzed a 3D buckling analysis of FGM sandwich plates under bi-axial compressive loads. Chen (2018) studied the transfer matrix method for the solution of FGMs thick-walled cylinders with an arbitrary inhomogeneous elastic response. Arefi (2015) presented the effect of different functionalities of FGM and FGPM layers on free vibration analysis of the FG circular plates integrated with piezoelectric layers. Ebrahimi and Barati (2016) analyzed a nonlocal higher-order shear deformation beam theory for vibration analysis of size-dependent functionally graded. Panda and Chandran (2003) analyzed the titanium-titanium boride (Ti-TiB) functionally graded materials through reaction sintering. Avcar and Mohammed (2018) studied the free vibration of functionally graded beams resting on the Winkler-Pasternak foundation.

A refined theory of shear of higher order and normal deformation for the plates E-, P- and S-FGM on the elastic foundations Pasternak proposed by Lee *et al*. (2015), where it could present strong similarities with the classic theory of the plates in many aspects such as the boundary conditions, the equation of motion and the resulting expressions of the stresses.

Radwan and Zenkour (2018) studied a quasi 3D trigonometric theory, the effects of Winkler and Pasternak parameters, the ratio (dimension/thickness), the inhomogeneity parameter, and the aspect ratio on the bending responses of FG plates. They also studied the flexural and free vibration compression of functionally graded plates and multilayer composite sandwich plates with a flexible core on Winkler-Pasternak foundations.

A new quasi-3D hyperbolic shear deformation theory for bending and free vibration of FG plates is presented by Khiloun *et al*. (2019) where they demonstrate that the theory presented is not only accurate but also effective in predicting displacements, stresses and the natural frequency of homogeneous plates and FG. Thai and Kim (2013) presented a quasi 3D sinusoidal shear strain theory with only five unknowns to study the behavior of plates in FGM bending. Two types of higher-order kinematic theories are adopted by Hirwani *et al*. (2018b) to evaluate the nonlinear bending and the stress values of the internally damaged layered composite flat panel structure numerically including the thickness stretching effect. The results of this study has been validated with available published theoretical and experimental results.

Baferani and Saidi (2013) accurate solution for free vibration analysis of FG thick rectangular plates resting on elastic foundation. Dorduncu (2019) think about the flexure analysis of FG plates using refined zigzag theory, where it was observed that the material variation through the thickness played a major role in the stress and displacement levels whilst the influence of the material variation was minor on the stress and displacement profiles. Vel and Batra (2003) presented the thermoelasticity exact solution for cylindrical bending deformations of functionally graded plates. Ebrahimi and Daman (2017) presented a nonlocal thermo-electromechanical vibration analysis of smart curved FG piezoelectric Timoshenko nanobeam.

Nguyen *et al*. (2019) presented a simple refined (FSDT) for free vibration, static and bending analysis of advanced composite plates which this theory can be applied to the studied other structures such as beams and shells in advanced composite plates. Amir *et al*. (2019) studied the size-dependent magneto-electro-elastic vibration analysis of FG saturated porous annular/circular micro sandwich plates embedded with nano-composite face sheets subjected to multi-physical preloads. Beldjelili *et al*. (2016) have studied the Hygro-thermo-mechanical bending of S-FGM plates resting on a variable elastic foundation using a four-variable trigonometric plate theory. They were able to demonstrate that the deflection and stresses obtained by the proposed theory with four unknowns are almost identical to those given by other shear deformation theories containing five unknowns.

The static analysis of thick functionally graded plates with different property distribution functions is presented by Ghazzawi and Abdelrahman (2020), the purpose of the model used by these authors is to study the effect of shear deformation on the bending behavior of the plate for different values of the plate aspect ratio, thickness ratio and modulus of elasticity ratio of the constituents.

Throughout the literature it is noted that the current methods are developed by taking particular account of the following assumptions: the materials are elastic and linear. In addition, the beam or the plate FGM is orthotropic at any point of structure.

Since the not exist of experimental methods for predicting the bending of FGM structures under stretching effect, the continuum mechanics methods are often used to investigate some physical problems of the materials. The objective of the present paper is to study the mechanical behavior of Functionally Graduated Plates using a new theory of quasi-3D shear deformation that takes into account the stretching effect of thickness. The numerical results presented in this study will serve as a reference for the use and development of FGM materials.

2. Kinematics and constitutive equations

2.1 Field of displacements

Based on the assumptions made in the introduction section, the Displacement field can be obtained using the following equations

$$u_1(x,y,z,t) = u(x,y,t) - z\frac{\partial w_0(x,y,t)}{\partial x} + f(z)\phi_x(x,y,t) \tag{1a}$$

$$u_2(x,y,z,t) = v(x,y,t) - z\frac{\partial w_0(x,y,t)}{\partial y} + f(z)\,\phi_y(x,y,t) \tag{1b}$$

$$u_3(x,y,z,t) = w_0(x,y,t) + g(z)\,\theta_3(x,y,t) \tag{1c}$$

Where

$$\phi_x(x,y,t) = k_1\int \theta(x,y,t)dx \tag{2a}$$

$$\phi_y(x,y,t) = k_2\int \theta(x,y,t)dy \tag{2b}$$

By substituting the expressions of ϕ_x, *and* ϕ_y from Eqs. (2) into Eq. (1) the following equations are obtained.

$$u_1(x,y,z,t) = u(x,y,t) - z\frac{\partial w_0(x,y,t)}{\partial x} + k_1 f(z)\int^{\int} \theta(x,y,t)\,dx \tag{3a}$$

$$u_2(x,y,z,t) = v(x,y,t) - z\frac{\partial w_0(x,y,t)}{\partial y} + k_2 f(z)\int^{\int} \theta(x,y,t)\,dy \tag{3b}$$

$$u_3(x,y,z,t) = w_0(x,y,t) + g(z)\,\theta_3(x,y,t) \tag{3c}$$

Where (u_1, u_2, u_3) are the displacement in (x, y, z) coordinate directions respectively. u and v are the displacement in the x and y coordinate directions at a point on the mid-surface of the plate. w_0 and θ are the bending and the shear components of the transverse displacement respectively. h is the thickness of the plate. In additional, $\theta_3(x, y)$ is an unknown displacement function accounting for the thickness stretching effect. The shape functions $f(z)$ and $g(z)$ are chosen based on a third order shear deformation theory and the stress-free boundary conditions on the top and bottom surfaces of the plate respectively as

$$g(z) = \frac{df(z)}{dz} \tag{4}$$

$$f(z) = z\left(\frac{5}{4} - \frac{5z^2}{3h^2}\right) \tag{5}$$

The deformations associated with the displacement field in Eq. (3) are as follows

$$\begin{Bmatrix}\varepsilon_x\\ \varepsilon_y\\ \gamma_{xy}\end{Bmatrix} = z\begin{Bmatrix}k_x^b\\ k_y^b\\ k_{xy}^b\end{Bmatrix} + f(z)\begin{Bmatrix}k_x^s\\ k_y^s\\ k_{xy}^s\end{Bmatrix} \tag{6}$$

$$\begin{Bmatrix}\gamma_{yz}\\ \varepsilon_{xz}\end{Bmatrix} = g(z)\begin{Bmatrix}\gamma_{yz}^0\\ \gamma_{xz}^0\end{Bmatrix} \tag{7}$$

$$\varepsilon_{zz} = g'(z)\varepsilon_z^0 \tag{8}$$

$$\begin{Bmatrix}\varepsilon_{xx}^0\\ \varepsilon_{yy}^0\\ \gamma_{xy}^0\end{Bmatrix} = \begin{Bmatrix}\dfrac{\partial u_0}{\partial x}\\ \dfrac{\partial v_0}{\partial y}\\ \dfrac{\partial u_0}{\partial y} + \dfrac{\partial v_0}{\partial x}\end{Bmatrix} \tag{9}$$

$$\begin{Bmatrix}k_{xx}^b\\ k_{yy}^b\\ k_{xy}^b\end{Bmatrix} = \begin{Bmatrix}-\dfrac{\partial^2 w_0}{\partial x^2}\\ -\dfrac{\partial^2 w_0}{\partial y^2}\\ -2\dfrac{\partial^2 w_0}{\partial x\partial y}\end{Bmatrix} \tag{10}$$

$$\begin{Bmatrix}k_{xx}^s\\ k_{yy}^s\\ k_{xy}^s\end{Bmatrix} = \begin{Bmatrix}k_1\theta\\ k_2\theta\\ k_1\dfrac{\partial}{\partial y}\displaystyle\int \theta dx + k_2\frac{\partial}{\partial x}\int \theta dy\end{Bmatrix} \tag{11}$$

$$\begin{Bmatrix}\gamma_{yz}^0\\ \gamma_{xz}^0\end{Bmatrix} = \begin{Bmatrix}k_2\displaystyle\int \theta\,dy + \frac{\partial\theta_3}{\partial y}\\ k_1\displaystyle\int \theta\,dx + \frac{\partial\theta_3}{\partial x}\end{Bmatrix} \tag{12}$$

$$\varepsilon_z^0 = \theta_3 \tag{13}$$

The integrals used in the above equations must be solved by a Navier-type solution and can be expressed as follows

$$\frac{\theta}{\partial y}\int \theta dx = A_1 \frac{\partial^2 \theta}{\partial x \partial y}, \qquad \frac{\theta}{\partial x}\int \theta dx = B_1 \frac{\partial^2 \theta}{\partial x \partial y} \tag{14}$$

$$\int \theta dx = A_1 \frac{\partial \theta}{\partial x}, \qquad \int \theta dy = B_1 \frac{\partial \theta}{\partial y} \tag{15}$$

Where the coefficients A_1 and B_1 are determined according to Navier-type solution. Therefore, A_1, B_1, k_1 and k_2 are expressed as follows

$$A_1 = -\frac{1}{\xi^2}, \quad B_1 = -\frac{1}{\eta^2}, \quad k_1 = \xi^2, \quad k_2 = \eta^2 \tag{16}$$

where ξ and η are defined in the equations

$$\xi = \frac{m\pi}{a}, \quad \eta = -\frac{m\pi}{b} \tag{17}$$

The constitutive relations of a *FG* plate can be written as

$$\begin{Bmatrix} \sigma_{xx} \\ \sigma_{yy} \\ \sigma_{zz} \\ \tau_{xy} \\ \tau_{yz} \\ \tau_{xz} \end{Bmatrix} = \begin{Bmatrix} Q_{11} & Q_{12} & Q_{12} & 0 & 0 & 0 \\ Q_{12} & Q_{11} & Q_{11} & 0 & 0 & 0 \\ Q_{12} & Q_{12} & Q_{11} & 0 & 0 & 0 \\ 0 & 0 & 0 & Q_{66} & 0 & 0 \\ 0 & 0 & 0 & 0 & Q_{44} & 0 \\ 0 & 0 & 0 & 0 & 0 & Q_{55} \end{Bmatrix} \begin{Bmatrix} \varepsilon_{xx} \\ \varepsilon_{yy} \\ \varepsilon_{zz} \\ \gamma_{xy} \\ \gamma_{yz} \\ \gamma_{xz} \end{Bmatrix} \tag{18}$$

Where Q_{ij} are the three-dimensional elastic constants

$$\begin{aligned} Q_{11}(z) &= E(z)(1-\nu)/(1-2\nu)(1+\nu) \\ Q_{12}(z) &= E(z)\nu/(1-2\nu)(1+\nu) \end{aligned} \tag{19}$$

$$\begin{aligned} Q_{66}(z) &= \frac{E(z)}{2(1+\nu)} \\ Q_{44}(z) &= Q_{55}(z) = Q_{66}(z) \end{aligned} \tag{20}$$

2.2 Constitutive relations of FGM structures

The production of functional gradation materials is carried out by varying the constituents of the materials to have mechanical properties which change continuously over the thickness of the structures. Each FGM product can be defined by the variation of volume fractions. Often, we use the power law function, the exponential function or the sigmoid function to describe the fractions of volume.

2.2.1 Exponential function (*E-FGM*)

In this method, the volume fraction is given as an exponential function across the thickness

$$E(z) = Ae^{B\left(z+\frac{h}{2}\right)} \tag{21}$$

With

$$A = E_2, \qquad B = \frac{1}{h}\ln(E_1/E_2) \tag{22}$$

Where h is the thickness of the plate and E_2 present the Young's modulus of the homogeneous face of the plate. B is the index of the material variation across the thickness of the plate.

2.2.2 Powers -Law function (*P-FGM*)

The volume fraction of the ceramic constituent of the *FG* plate is supposed to be given by

$$V_1(z) = \left(\frac{z+h/2}{h}\right)^p \tag{23}$$

Where p is the material parameter that dictates the material variation profile through the thickness.

The local volume fraction $V_1(z)$ has been defined, the material properties of a *P-FGM* can be determined by the rule of mixture.

$$E(z) = V_1(z)E_1 + (1 - V_1(z))E_2 \tag{24}$$

2.2.3 Sigmoid function (*S-FGM*)

The volume fraction using two power-law functions which ensure smooth distribution of stresses is defined.

$$V_1(z) = 1 - \frac{1}{2}\left(\frac{\frac{h}{2}-z}{\frac{h}{2}}\right)^p, \quad V_2(z) = \frac{1}{2}\left(\frac{h/2+z}{h/2}\right)^p \tag{25}$$

The mixing rule allows us to calculate the material properties of S-FGM which is

$$\begin{aligned} E(z) &= V_1(z)E_1 + \big(1 - V_1(z)\big)E_2 \ \text{ for } \ 0 < z < h/2 \\ E(z) &= V_2(z)E_1 + \big(1 - V_2(z)\big)E_2 \ \text{ for } -h/2 < z < 0 \end{aligned} \tag{26}$$

3. Elastic medium models

The FGM plate is put in an elastic medium, which is expected to involvement vertical displacement but no horizontal displacement. The density of the reaction force at the FGM plate bottom can be communicated by two models.

3.1 Winkler model

In the case of Winkler foundation model, the distributed load can be defined by

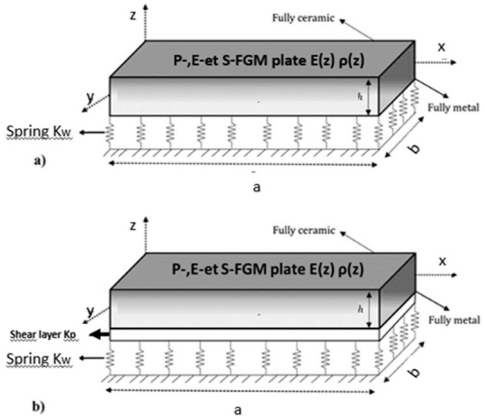

Fig. 1 FGM plate on Pasternak's elastic medium

$$q_{winkler} = k_w u_3 = k_w(w_0 + g(z)\theta_3) \tag{27}$$

where k_w is the constant of proportionality that is referred to as the modulus of medium reaction (so-called spring constant).

3.2 Pasternak model

The Pasternak model foundation is a two-parameter elastic model, which consists of a shear layer parameter with stiffness k_p (physically, this parameter depicts the interaction owing to shear action among the spring parts) and independent upper spring with stiffness k_w (Winkler model). So, the distributed reaction between Pasternak foundation model and the lower surface of FGM plate can be defined by Shahsavari *et al*. (2018)

$$\begin{aligned} &q_{Pasternak} \\ &= k_w\big(w_0(x,y,t) + g(z)\theta_3(x,y,t)\big) \\ &\quad + k_p\nabla^2\big(w_0(x,y,t) + g(z)\theta_3(x,y,t)\big) \\ &q_{Pasternak} \\ &= k_w(w_0(x,y,t) + g(z)\theta_3(x,y,t)) \\ &\quad + k_{px}\frac{\partial^2}{\partial x^2}(w_0(x,y,t) + g(z)\theta_3(x,y,t)) \\ &\quad + k_{py}\frac{\partial^2}{\partial y^2}(w_0(x,y,t) + g(z)\theta_3(x,y,t)) \end{aligned} \tag{28}$$

Where ($\nabla^2 = \partial^2/\partial x^2 + \partial^2/\partial y^2$) expresses the Laplace differential operator in rectangular Cartesian coordinates.

4. Equilibrium equations

4.1 The Hamilton principle

Hamilton's principle is used here in to derive the equations of motion. The principle can be stated in analytical form as

$$\begin{aligned} \delta U &= \int_A \int_{-h/2}^{h/2} \sigma_{xx}\,\delta\varepsilon_{xx} + \sigma_{yy}\delta\varepsilon_{yy} + \sigma_{zz}\delta\varepsilon_{zz} \\ &\qquad + \sigma_{xy}\delta\gamma_{xy} + \sigma_{yz}\delta\gamma_{yz} + \sigma_{xz}\delta\gamma_{xz})dzdA \\ &= \int_A N_x\,\delta\varepsilon_x^0 + N_y\delta\varepsilon_y^0 + N_z\delta\varepsilon_z^0 + N_{xy}\delta\gamma_{xy}^0 \\ &\quad + M_x^b\delta k_x^b + M_y^b\delta k_y^b + M_{xy}^b\delta k_{xy}^b + M_x^s\delta k_x^s \\ &\quad + M_x^s\delta k_x^s + M_{xy}^s\delta k_{xy}^s + S_{yz}^s\delta\gamma_{yz}^0 + S_{xz}^s\delta\gamma_{xz}^0)dA \end{aligned} \tag{29}$$

Where δu, δ and A are the variation of strain energy, a variational operator and the top surface respectively.

The stress resultants N, M, and S are expressed by

$$(N_i, M_i^b, M_i^s) = \int_{-\frac{h}{2}}^{\frac{h}{2}} (1, z, f)\,\sigma_i dz \quad (i = x, y, xy) \tag{30a}$$

$$N_z = \int_{-h/2}^{h/2} g'(z)\sigma_z dz \tag{30b}$$

$$(S_{yz}^s, S_{xz}^s) = \int_{-h/2}^{h/2} g\,(z)(\tau_{xz}, \tau_{yz})dz \tag{30c}$$

The first variation of the additional strain energy induced by the elastic medium can be expressed as

$$\begin{aligned} \delta U_m = \int_A \Big[& k_w u_3 \delta u_3 + k_p\left(\frac{\partial u_3}{\partial x}\left(\frac{\partial \delta u_3}{\partial x}\right)\right. \\ & \left. + \frac{\partial u_3}{\partial y}\left(\frac{\partial \delta u_3}{\partial y}\right)\right] dxdy \end{aligned} \tag{31}$$

Vertical load can be expressed using

$$\delta V = \int_A q_z\,\delta u_3 dxdy \tag{32}$$

Where, the vertical load q_z only at the top surface is considered.

The total potential energy principle was applied to derive the equilibrium equation (Khiloun *et al*. 2019).

$$\delta\Pi = \delta[(U + U_m) + V)] = 0 \tag{33}$$

Substituting the expressions for δU, δV, and δU_m from Eqs. (29), (31), and (32) into Eq. (33) and integrating by parts, and collecting the coefficients of the following equations of motion.

$$\delta u: \quad \frac{\partial N_x}{\partial x} + \frac{\partial N_{xy}}{\partial y} = 0 \tag{34a}$$

$$\delta v: \quad \frac{\partial N_y}{\partial y} + \frac{\partial N_{xy}}{\partial x} = 0 \tag{34b}$$

$$\begin{aligned} \delta w_0: \ & \frac{\partial}{\partial x}\left(\frac{\partial M_x^b}{\partial x} + \frac{\partial M_{xy}^b}{\partial y}\right) + \frac{\partial}{dy}\left(\frac{\partial M_y^b}{\partial y} + \frac{\partial M_{xy}^b}{\partial x}\right) \\ & + q_z + k_w(w_0(x,y,t) + g(z)\theta_3(x,y,t)) \\ & + k_P\nabla^2(w_0(x,y,t) + g(z)\theta_3(x,y,t)) = 0 \end{aligned} \tag{34c}$$

$$\begin{aligned} \delta\theta: \quad & k_1 M_x^s + k_1 M_y^s + (k_1 A_1 + \mathrm{k}_2 B_1)\frac{\partial^2 M_{xy}^s}{\partial x \partial y} \\ & - k_1 A_1 \frac{\partial S_{xz}^s}{\partial x} - k_2 B_1 \frac{\partial S_{yz}^s}{\partial y} = 0 \end{aligned} \tag{34d}$$

$$\begin{aligned} \delta\theta_3: \ & \frac{\partial S_{xz}^s}{\partial x} + \frac{\partial S_{yz}^s}{\partial y} \text{-g}(z)q_z + k_w\,g(z)\,(w0(x,y,t) \\ & + g(z)\theta_3(x,y,t)) + k_P g(z)\nabla^2(w0(x,y,t) \\ & + g(z)\theta_3(x,y,t)) = 0 \end{aligned} \tag{34e}$$

5. Analytical solutions

In this study, a simply supported rectangular plate was considered. The length, width, and height of the plate were a, b, and h respectively. The plate was subjected to a distributed transverse load q. employing the Navier solution, the solutions of the plate were assumed as

$$\begin{Bmatrix} u \\ v \\ w0 \\ \theta \\ \theta 3 \end{Bmatrix} = \sum_{m=1}^{\infty}\sum_{n=1}^{\infty} \begin{Bmatrix} U_{mn}e^{i\omega t}\,cos(\xi x)\,sin(\eta y) \\ V_{mn}e^{i\omega t}\,sin(\xi x)\,cos(\eta y) \\ W_{mn}e^{i\omega t}\,sin(\xi x)\,sin(\eta y) \\ X_{mn}e^{i\omega t}\,sin(\xi x)\,sin(\eta y) \\ Y_{mn}e^{i\omega t}\,sin(\xi x)\,sin(\eta y) \end{Bmatrix} \tag{35}$$

Where ω is the frequency of vibration.

The transverse distributed load q_z (x, y) was also expanded in the following form

$$q_z(x,y) = \sum_{m=1}^{\infty}\sum_{n=1}^{\infty} Q_{mn} W_{mn} sin(\xi x) sin(\eta y) \quad (36)$$

For the case of a sinusoidal distributed load, we have

$$Q_{mn} = q_0, \quad m = n = 1 \quad (37)$$

For the case of uniformly distributed load, the coefficients Q_{mn} are defined as follows

$$Q_{mn} = 16\, q_0/\mathrm{mn}\pi^2 \quad (38)$$

By substituting Eqs. (34) and (35) into the equations of motion. Eqs. (34a)-(34e), analytical solutions can be obtained from the following equation

$$\{K\}\{\Delta\} = \{Q\} \quad (39a)$$

$$\{\Delta\} = \{U_{mn},\ V_{mn},\ W_{mn},\ X_{mn},\ Y_{mn}\}^T \quad (39b)$$

$$\{Q\} = \{0,\ 0,\ Q_{mn},\ 0,\ g(z)Q_{mn}\}^T \quad (39c)$$

Where K, $\{Q\}$, and $\{\Delta\}$ are the stiffness matrix, the force vector and the vector of unknown coefficients respectively.

6. Numerical results and discussion

6.1 Material properties

In this panel the calculated displacements of the FGM plates, which are graduated from the lower surface to the upper surface according to Eq. (20), are provided and compared with the results of different theories presented by the authors. The material properties of the FG plates are given in Table 1.

The non-dimensional displacement components of these tables are

$$\overline{W} = \frac{10E_1h^3}{q_0a^4} W\left(\frac{a}{2},\ \frac{b}{2},\ z\right) \quad (40)$$

$$D_0 = \frac{E_1h^3}{12}, \quad E_0 = 1.0\ \mathrm{Gpa} \quad (41)$$

$$\hat{W} = \frac{100D_0}{q_0a^4} W\left(\frac{a}{2},\ \frac{b}{2},\ z\right) \quad (42)$$

Table 1 Material properties of FGM Plate

Proprieties	Metal	Ceramic
	Aluminum (Al)	Alumina (Al_2O_3)
Elastic modulus: E (Gpa)	70	380
Poisson's ratio: ν	0.3	0.3
Masse density: ρ (kg/m^3)	2702	3800

$$k_w = \frac{k_0E_0h^3}{a^4}, \quad k_{px} = \frac{j_0E_0h^3\upsilon}{a^2}, \quad k_{py} = \frac{j_0E_0h^3\upsilon}{b^2} \quad (43)$$

$$D_m = \frac{E_2h^3}{12(1-\upsilon^2)} \quad (44)$$

$$K_w = \frac{\overline{k}_wD_m}{a^4}, \quad K_p = \frac{\overline{k}_pD_m}{a^2} \quad (45)$$

6.2 Validation of proposed theory

To enable us to demonstrate the accuracy of the proposed theory for the study of the bending responses of simply supported FG plates, numerical examples are presented for comparison with the results of different 3D, quasi-3D and 2D shear deformation theories.

In Table 2 shows the maximum non-dimensional deflection $\overline{W}$ of a square plate P-FGM subjected to a sinusoidal load for different values of the thickness ratio a/h. Three different values of the power-law index p = 1, p = 4 and p = 10 were used in this example. The results obtained are compared with the results determined by the authors (Lee *et al*. 2015, Yi *et al*. 2017, Zenkour and Alghanmi 2018, Zenkour and Radwan 2018b, Khiloun *et al*. 2019 and Nguyen *et al*. 2019). When the side-to-thickness ratio is 100, the values of the transverse displacements are

Table 2 Comparison of nondimensional deflection ($\overline{W}$) of Al/AL_2O_3 square P-FGM plate

p	Theory	a/h		
		4	10	100
1	Lee *et al*. (2015)	0,6916	0,5696	0,5462
	Yi *et al*. (2017)	0,7318	0,5891	0,5625
	Zenkour and Alghanmi (2018)	0,6828	0,5592	0,5459
	Zenkour and Radwan (2018)	0.7284	0.5889	0.5625
	Khiloun *et al*. (2019)	0,7289	0,5890	0,5625
	Nguyen *et al*. (2019)	0.7177	0.5872	0.5625
	Present	0,6916	0,5696	0,5462
4	Lee *et al*. (2015)	1,0984	0,8424	0,7934
	Yi *et al*. (2017)	1,1732	0,8831	0,8287
	Zenkour and Alghanmi (2018)	1,1001	0,8404	0,7933
	Zenkour and Radwan (2018)	1.1573	0.8810	0.8287
	Khiloun *et al*. (2019)	1,0964	0,8413	0,7926
	Nguyen *et al*. (2019)	1.1028	0.8721	0.8286
	Present	1,0984	0,8424	0,7934
10	Lee *et al*. (2015)	1,3357	0,9817	0,9140
	Yi *et al*. (2017)	1,3333	0,9791	0,9114
	Zenkour and Alghanmi (2018)	1,3391	0,9806	0,9139
	Zenkour and Radwan (2018)	1.3889	1.0083	0.9362
	Khiloun *et al*. (2019)	1,4026	1,0094	0,9362
	Nguyen *et al*. (2019)	1.3796	1.0065	0.9362
	Present	1,3357	0,9817	0,9140

Table 3 Comparison of nondimensional deflection ($\overline{W}$) of Al/AL_2O_3 square P-FGM plate

b/*a*	Theory	Power law index (*p*)					
		0.1	0.3	0.5	0.7	1	1.5
1	Mantari and Soares (2013)	0,5779	0,5224	0,4717	0,4256	0,3648	0,2793
	Fekrar *et al*. (2014)	0.5730	0.5180	0.4678	0.4221	0.3611	0.2771
	Nguyen (2015)	0,6211	0,5615	0,5073	0,4579	0,3921	0,3014
	Lee *et al*. (2015)	0.5777	0.5222	0.4716	0.4255	0.3640	0,2793
	Adim and Daouadji (2016)	0,5780	0,5225	0,4719	0,4258	0,3642	0,2794
	Nguyen *et al*. (2019)	0.6692	0.6062	0.5460	0.4879	0.4003	0.2786
	Present	0,5303	0,5222	0.4716	0.4255	0.3640	0.2792
2	Mantari and Soares (2013)	1,1941	1,0795	0,9750	0,8799	0,7538	0,5786
	Fekrar *et al*. (2014)	1.1879	1.0739	0.9701	0.8754	0.7493	0.5757
	Nguyen (2015)	1,1939	1.0792	0.9748	0.8797	0.7529	0.5784
	Lee *et al*. (2015)	1,2569	1,1367	1,0275	0,9284	0,7965	0,6153
	Adim and Daouadji (2016)	1,1942	1,0796	0,9751	0,8800	0,7532	0,5786
	Nguyen *et al*. (2019)	1.3239	1.1928	1.0674	0.9454	0.7578	0.5958
	Present	1,1427	1.0792	0.9748	0.8797	0.7529	0.5784
3	Mantari and Soares (2013)	1,4421	1,3037	1,1776	1,0628	0,9104	0,6993
	Fekrar *et al*. (2014)	1.4354	1.2977	1.1722	1.0579	0.9056	0.6961
	Nguyen (2015)	1,4419	1,3035	1,1774	1,0626	0,9096	0,6991
	Lee *et al*. (2015)	1,5115	1,3671	1,2360	1,1169	0,9587	0,7414
	Adim and Daouadji (2016)	1,4422	1,3038	1,1777	1,0629	0,9098	0,6993
	Nguyen *et al*. (2019)	1,5843	1,4255	1,2734	1,1253	0,8965	0,6766
	Present	1,3892	1,3035	1,1774	1,0626	0,9096	0,6991

Table 4 Comparison of nondimensional deflection ($\overline{W}$) of E-FGM plate ($a/h = 4$)

b/*a*	Theory	Power law index (p)					
		0.1	0.3	0.5	0.7	1	1.5
1	Mantari and Soares (2013)	0,3111	0,2814	0,2546	0,2302	0,1980	0,1537
	Fekrar *et al*. (2014)	0.3474	0.3141	0.2838	0.2563	0.2196	0.1692
	Lee *et al*. (2015)	0,3486	0,3151	0,2847	0,2571	0,2202	0,1697
	Nguyen (2015)	0,3575	0,3235	0,2927	0,2649	0,2280	0,1775
	Nguyen *et al*. (2019)	0,3651	0,3257	0,2879	0,2507	0,1917	0,1088
	Present	0,3453	0,3152	0,2847	0,2571	0,2202	0,1697
2	Mantari and Soares (2013)	0,8144	0,7364	0,6654	0,6009	0,5150	0,3973
	Fekrar *et al*. (2014)	0.8120	0.7342	0.6635	0.5991	0.5136	0.3962
	Lee *et al*. (2015)	0,8145	0,7365	0,6655	0,6009	0,5151	0,3973
	Nguyen (2015)	0,8285	0,7498	0,6787	0,6145	0,5296	0,4135
	Nguyen *et al*. (2019)	0,8374	0,7440	0,6543	0,5659	0,5239	0,4240
	Present	0,8110	0,7364	0,6654	0,6009	0,5150	0,3973
3	Mantari and Soares (2013)	1,0124	0,9154	0,8272	0,7470	0,6403	0,4940
	Fekrar *et al*. (2014)	1.0093	0.9127	0.8247	0.7448	0.6385	0.4927
	Lee *et al*. (2015)	1,0281	0,9305	0,8424	0,7628	0,6576	0,5137
	Nguyen (2015)	1,0136	0,9154	0,8272	0,7470	0,6403	0,4940
	Nguyen *et al*. (2019)	1,0370	0,9205	0,8088	0,7985	0,6209	0,5708
	Present	1,0090	0,9154	0,8272	0,7470	0,6403	0,4940

Table 5 Comparison of nondimensional deflection ($\overline{W}$) of E-FGM plate (a/h = 10)

b/a	Theory	Power law index (p)					
		0.1	0.3	0.5	0.7	1	1.5
1	Thai and Kim (2013)	0.2790	0.2523	0.2280	0.2060	0.1767	0.1366
	Mantari and Soares (2013)	0,2799	0,2531	0,2287	0,2066	0,1772	0,137
	Lee *et al*. (2015)	0,2797	0,2531	0,2287	0,2066	0,1772	0,1369
	Adim and Daouadji (2016)	0,2799	0,2531	0,2287	0,2066	0,1772	0,137
	Present	0,2797	0,2531	0,2287	0,2066	0,1772	0,1369
2	Thai and Kim (2013)	0.7015	0.6344	0.5734	0.5180	0.4444	0.3435
	Mantari and Soares (2013)	0,7037	0,6364	0,5752	0,5196	0,4457	0,3445
	Lee *et al*. (2015)	0,7036	0,6364	0,5752	0,5196	0,4457	0,3445
	Adim and Daouadji (2016)	0,7037	0,6364	0,5752	0,5196	0,4457	0,3445
	Present	0,7036	0,6364	0,5751	0,5195	0,4457	0,3445
3	Thai and Kim (2013)	0.8849	0.8002	0.7233	0.6534	0.5605	0.4333
	Mantari and Soares (2013)	0,8877	0,8027	0,7255	0,6554	0,5622	0,4346
	Lee *et al*. (2015)	0,8877	0,8027	0,7255	0,6554	0,5622	0,4346
	Adim and Daouadji (2016)	0,8877	0,8027	0,7255	0,6554	0,5622	0,4346
	Present	0,8875	0,8027	0,7255	0,6554	0,5622	0,4346

almost the same as the values presented by the authors cited above.

Analyzing Table 2, it can be noticed that the results obtained under the effect of thickness stretching are in good agreement with the published results available in the reference for thin and thick FGM plates. Continuously, an exponential plate of E-FGM with a thickness ratio a/h = 2, 4 and 10 subjected to sinusoidal loads is analyzed. The Young's modulus was evaluated using the exponential distribution.

The non-dimensional displacements are given in Table 3-5 for different values of the aspect ratio b/a, the thickness ratio a/h and the exponential value p. The results of the present theory were compared with those of the FSDT solution (Nguyen *et al*. 2019), the quasi-3D theories (Thai and Kim 2013, Adim and Hassaine Daouadji 2016), the HSDT (Lee *et al*. 2015, Mantari and Soares 2013, Fekrar *et al*. 2014). The models presented and other quasi-3D models introducing the influence of thickness, the results are close to each other. Meanwhile, 2D HSDT's that do not introduce

Table 6 Comparison of non-dimensional deflection ($\widehat{W}$) of P-FGM plates under uniform loads (a/h = 10, b/a = 3)

k_0	j_0	Theory	p				
			0	0,5	1	2	5
0	0	Zenkour (2009)	1,2582	1,9344	2,5133	3,2267	3,8517
		Lee *et al*. (2015)	1,2544	1,9045	2,4354	3,0816	3,6972
		Benahmed *et al*. (2017)	_	1.9021	_	3.0756	3.6937
		Present	1,2537	1,9036	2,4353	3,0834	3,7021
100	0	Zenkour (2009)	1,2582	1,9344	2,5133	3,2267	3,8517
		Lee *et al*. (2015)	1,2224	1,8317	2,3176	2,8951	3,4315
		Benahmed *et al*. (2017)	_	1.9021	_	3.0756	3.6937
		Present	1.2238	1.8355	2.3249	2.9086	3.4531
0	100	Zenkour (2009)	1,1661	1,7247	2,1701	2,6814	3,0979
		Lee *et al*. (2015)	1,1633	1,7019	2,1133	2,5825	2,9999
		Present	1,1682	1,7131	2,1321	2,6129	3,0441
100	100	Zenkour (2009)	1,1381	1,6639	2,0745	2,5364	2,9051
		Lee *et al*. (2015)	1,1136	1,6430	2,0230	2,4484	2,8197
		Benahmed *et al*. (2017)	_	1.6413	_	2.4446	2.8178
		present	1,1422	1,6578	2,0470	2,4864	2,8737

the influence of thickness stretching overestimate the results. In view of the above, it can be concluded that the introduction of the stretching effect of the plate thickness makes the FGM plate stiffer and leads to a reduction of the maximum total deflection $\overline{W}$.

In Table 6 Moderately thick rectangular plates of P-FGM are studied on a two-parameter elastic basis. The thickness ratio $a/h = 10$ and $b/a = 3$. In this section, the non-dimensional deformations of the P-FGM rectangular plates under uniform loads are studied. The deformations are presented for different values of the power law index p and the foundation parameters k_0, j_0 which vary from 0 and 100. The results presented in this section show that the studies made by Zenkour (2009) overestimate the deformations because of the thickness stretching effect, which is not taken into account in their theories.

6.3 Parameter studies

In the example of Fig. 4, a square plate in Al/Al_2O_3 has been considered is subject to a sinusoidal load. Young's modulus for Al was 70 GPa and 380 GPa for Al_2O_3, the Poisson ratios were constant for both and equal to 0.3, Power law index $p = \ln(E_1 / E_2)$ and $\overline{k_w} = 0$, $\overline{k_p} = 0$ (Winkler and Pasternak parameters).

The results obtained with this theory coincide with those presented with the solutions given by Lee *et al*. (2015). If we also analyze graph 4, we can see that the deflection decreases with the growth of the a/h ratio and becomes constant for $a/h > 20$, it is not very different for the two P- and E-FGM plates but more important than the S-FGM plate because the latter is more rigid (different mixing law) than the other plates. In this part, the effect of the elastic foundations is not taken into account, which explains the high value of the deflection. In Fig. 5 relates to the extent of the arrows in the center of the different plates P- FGM, E-FGM and S-FGM, of square shape, subjected to sinusoidal loads for $p = \ln(E_1 / E_2)$, and $\overline{k_w} = 0$, $\overline{k_p} = 0$. After analysis, we can see that the arrows in the center of the P-FGM plates are larger than those of the E-FGM and S-FGM plates. We can also notice that the values of the arrows determined for all the plates are less important than those calculated by Lee *et al*. (2015).

In the example of Figs. 6 to 8, a square plate in Al/Al_2O_3 has been considered is subject to a sinusoidal load. Young's modulus for Al was 70 GPa and 380 GPa for Al_2O_3, the Poisson ratios were constant for both and equal to 0.3, Power law index $p = \ln(E_1 / E_2)$ and, $(\overline{k_w}) = 0$ and 1000 $\overline{k_p} = 0$ and 100).

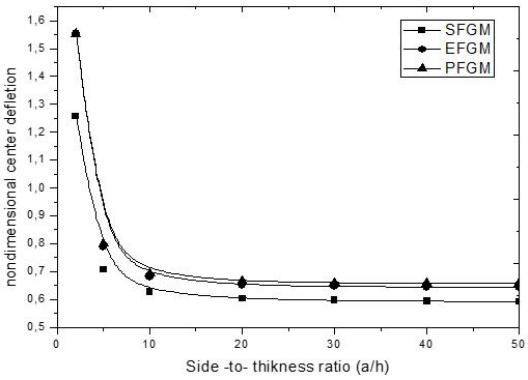

Fig. 4 Effect of side-to-thickness ratio (a/h) on nondimensional deflection of FGM thick plates ($p = \ln(E_1/E_2)$, ($b = a$, $\overline{k_w} = 0$, $\overline{k_p} = 0$)

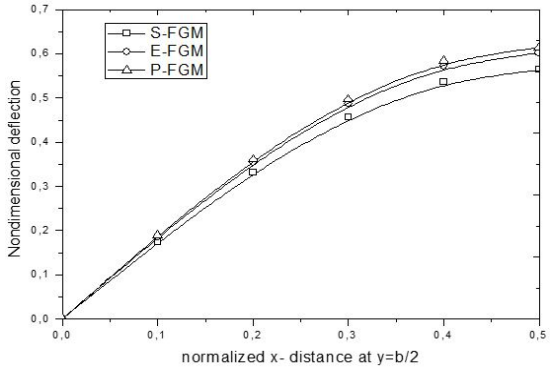

Fig. 5 The comparison of the deflection of E-FGM, P-FGM and S-FGM thick plates ($b = a$, $a/h = 10$, $\overline{k_w} = 0$, $\overline{k_p} = 0$)

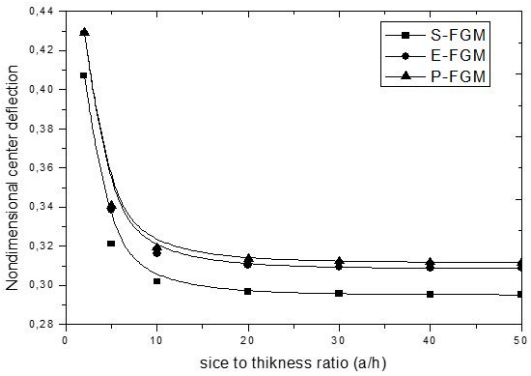

Fig. 6 Effect of side-to-thickness ratio (a/h) on nondimensional deflection of FGM thick plates ($b = a$, $\overline{k_w} = 1000$, $\overline{k_p} = 0$)

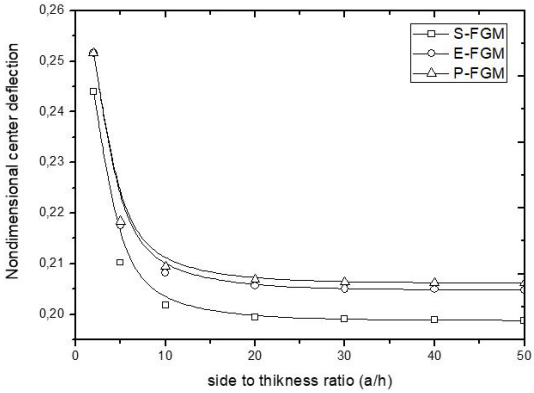

Fig. 7 Effect of side-to-thickness ratio (a/h) on nondimensional deflection of FGM thick plates ($b = a$, $\overline{k_w} = 0$, $\overline{k_p} = 100$)

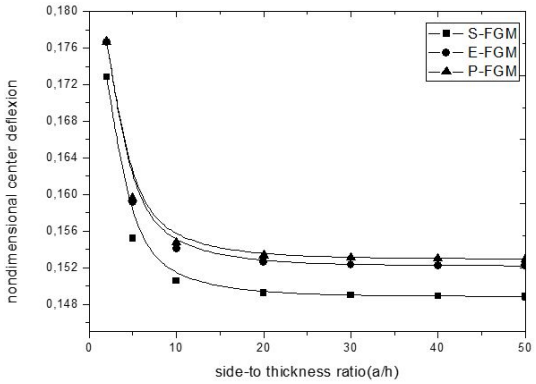

Fig. 8 Effect of side-to-thickness ratio (a/h) on nondimensional deflection of FGM thick plates ($p = \ln(E_1/E_2)$, ($b = a$, $\overline{k_w} = 1000$, $\overline{k_p} = 100$)

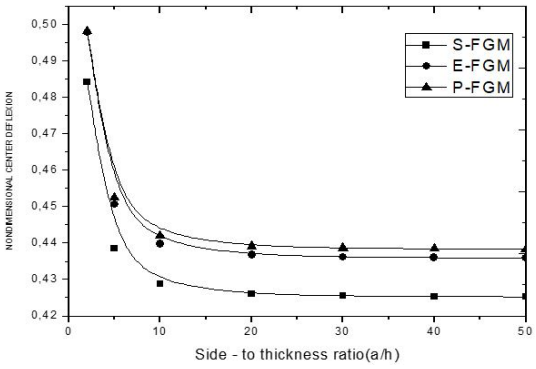

Fig. 9 Effect of side-to-thickness ratio (a/h) on nondimensional deflection of FGM thick plates ($b = 2a$, $\overline{k_w} = 1000$, $\overline{k_p} = 0$)

We can see that the deformation is important when the a/h ratio is low, but it is negligible when the side to thickness ratio becomes more important. It should be noted that the non-dimensional deflection, whatever the nature of the plate (P-, E- and S-FGM), decreases with the parameters of the elastic medium of Winkler and Pasternak. This decrease varies for $a/h = 20$ from half to a quarter compared to the plate without elastic foundation. These results are in agreement with those of Lee *et al*. (2015).

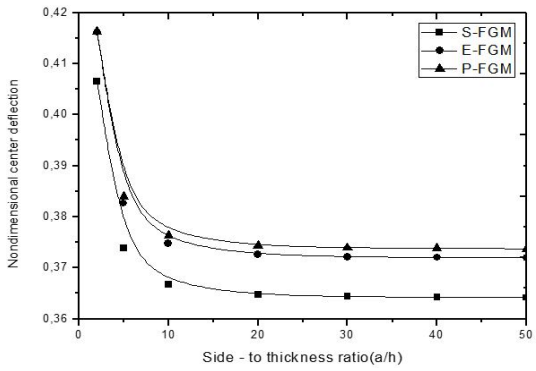

Fig. 10 Effect of side-to-thickness ratio (a/h) on nondimensional deflection of FGM thick plates ($b = 2a$, $\overline{k_w} = 0$, $\overline{k_p} = 100$)

After analysis of the various graphs (see synthesis in Table 7) relating to the study of the nondimensional bending of the P-, E-, and S-FGM plates as a function of the ratio a/h, a/b and the parameters $\overline{k_w}$ and, $\overline{k_p}$, we have observed that the transverse displacements are reduced during the existence of the elastic foundation.

The figures clearly show that the shear layer stiffness of the foundation (Pasternak parameter $\overline{k_p}$ is more effective than Winkler's $\overline{k_w}$ for reducing displacements. It was also found that:

- $\bar{w}\left(\overline{k_w} = 1000, \overline{k_p} = 100\right) \approx 20\%$ to $25\% \bar{w}\left(\overline{k_w} = 0, \overline{k_p} = 0\right)$ for $b = a,\ a/h = 5,$ $a/h = 20$
- $\bar{w}\left(\overline{k_w} = 1000, \overline{k_p} = 100\right) \approx 12\%$ to $14\% \bar{w}\left(\overline{k_w} = 0, \overline{k_p} = 0\right)$ for $b = 2a,\ a/h = 5,$ $a/h = 20$

To analyze the effect of the elastic foundation medium on the deflection we have as an example a S-FGM plate with the elastic parameters $\overline{k_w}$ and, $\overline{k_p}$, $p = \ln(E_1 / E_2)$ and $a/h = 0$. Figs. 12 and 13 show the effect of the elastic parameters Winkler and Pasternak on the deflection of an SFGM plate. Through this example, it is confirmed that the parameter of the elastic medium of Pasternak has more

Table 7 Effect of side-to-thickness ratio (a/h = 5 and 20) on nondimensional deflection of FGM plates ($a = b$, $a = 2b$, $p = \ln(E_1/E_2(\overline{k_w}) = 0$ and 1000 ($\overline{k_p}$) = 0 and 100)

b/a	$\overline{k_w}$	$\overline{k_p}$	$a/h = 5$			$a/h = 20$		
			S-FGM	E-FGM	P-FGM	S-FGM	E-FGM	P-FGM
1	0	0	0.7066	0.7886	0.8003	0.6023	0.6514	0.6652
	1000	0	0.3212	0.3384	0.3405	0.2967	0.3104	0.3135
	0	100	0.2102	0.2175	0.2184	0.1995	0.2056	0.2069
	1000	100	0.1552	0.1591	0.1596	0.1492	0.1526	0.1534
2	0	0	1.6848	1.8785	1.9105	1.5137	1.6588	1.6942
	1000	0	0.4385	0.4506	0.4524	0.4260	0.4367	0.4391
	0	100	0.3739	0.3826	0.3839	0.3647	0.3726	0.3743
	1000	100	0.2293	0.2325	0.2330	0.2258	0.2288	0.2294

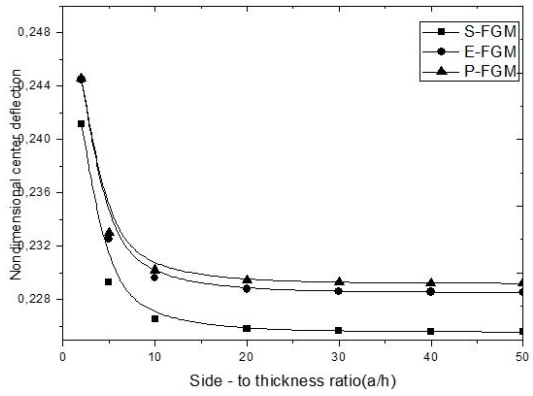

Fig. 11 Effect of side-to-thickness ratio (a/h) on nondimensional deflection of FGM thick plates ($b = 2a$, $\overline{k_w}$ = 1000, $\overline{k_p}$ = 100)

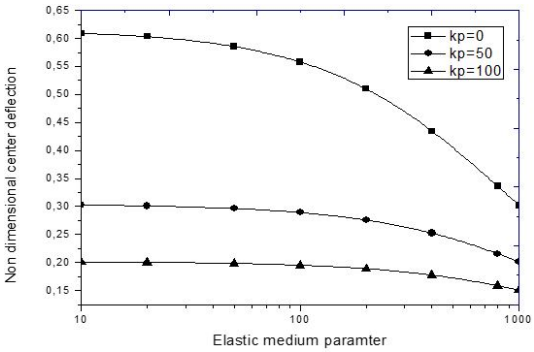

Fig. 12 Effect of elastic foundation parameter $\overline{k_w}$ on nondimensional deflection of S-FGM thick plates (a/h = 10, $\overline{k_p}$ = 0, 50, 100)

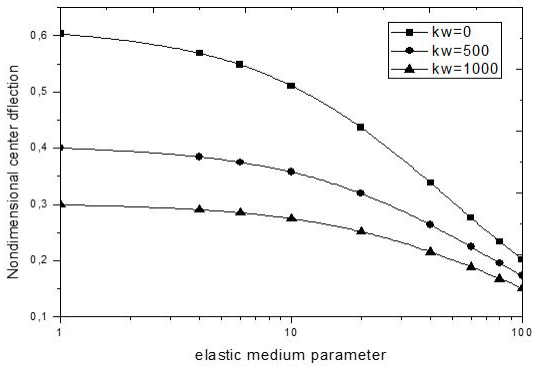

Fig. 13 Effect of elastic foundation parameter $\overline{k_p}$ on nondimensional deflection of S-FGM thick plate ((a/h = 10, $\overline{k_w}$ = 0, 500, 1000)

effect on the decrease of the non-dimensional deflection than the parameter of the elastic medium of Winkler

The effect of side to thickness ratio (a/h) on nondimensional deflection of S-FGM thick plates with power law index (p) (p = 1, 2, 5, 10, $\overline{k_w}$= 1000, ($\overline{k_p}$= 100), is studied in Fig. 14 where it can be seen that the non-dimensional deflection of an S-FGM plate resting on an average Winkler-Pasternak elastic, is almost constant for

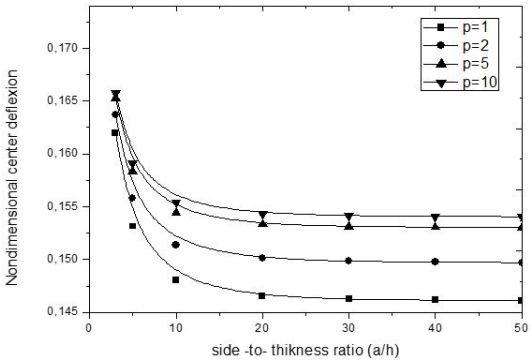

Fig. 14 Effect of side to thickness ratio (a/h) on nondimensional deflection of S-FGM thick plates with power law index (p) (p = 1, 2, 5, 10 $\overline{k_w}$ = 1000, $\overline{k_p}$ = 100)

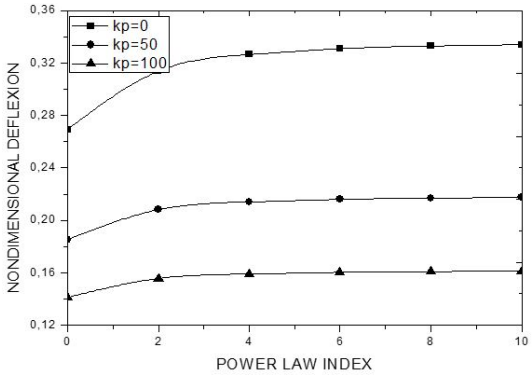

Fig. 15 Effect of power law index on nondimensional deflection of S-FGM thick plates (a/h = 10, $\overline{k_w}$ = 1000, $\overline{k_p}$ = 0, 50, 100)

ratio (a/h > 20). Also, it was found that when the power law index p > 5, the variation of the non-dimensional deflection becomes very small. In Fig. 15, the effect of the power law index on the non-dimensional deflection of the S-FGM plates is studied (a/h = 10, $\overline{k_w}$= 1000, $\overline{k_p}$= 0, 50, 100) and it is well confirmed that when the power law index p > 5, the variation in the deflection is negligible or even constant.

7. Conclusions

In this paper, a new quasi-3D theory for the study of the bending of functionally graduated plates for E-, P- and S-FGM thick plates on a Pasternak elastic base has been developed. Analytical solutions of simply supported plates are presented. Numerical results show that the present theory gives a very good prediction of bending. To test the convenience and accuracy of this proposed theory, analytical numerical examples were studied. According to these examples, the following noteworthy information was observed:

- It was observed from the comparative studies that quasi-3D theories that take into account thickness stretching effects can predict bending behavior more

accurately than other HSDT theories.
- The kinematics of the current theory is modified by considering indeterminate integral terms in the fields of displacements, which results in a reduced number of variables
- The proposed quasi-3D HSDT contains five unknowns, but gives results comparable to those predicted by existing quasi-3D theories that have more unknowns.

The numerical results presented in this paper can be used as a reference for the study and analysis of the flexural mechanical response of thick FGM plates resting on elastic foundations

Acknowledgments

Authors would like to acknowledge the support provided by the Directorate General for Scientific Research and Technological Development (DGRSDT).

References

Abdelmalek, A., Bouazza, M., Zidour, M. and Benseddiq, N. (2017), "Hygrothermal Effects on the Free Vibration Behavior of Composite Plate Using *n*th-Order Shear Deformation Theory: a Micromechanical Approach", *Iran. J. Sci. Technol. Transact. Mech. Eng.*, **43**(1), 61-73. https://doi.org/10.1007/s40997-017-0140-y

Adim, B. and Hassaine Daouadji, T. (2016), "Effects of thickness stretching in FGM plates using a quasi-3D higher order shear deformation theory", *Adv. Mater. Res., Int. J.*, **5**(4), 223-244. https://doi.org/10.12989/amr.2016.5.4.223

Amir, S., Arshid, E. and Arani, M.R.G. (2019), "Size-dependent magneto-electro-elastic vibration analysis of FG saturated porous annular/circular micro sandwich plates embedded with nano-composite face sheets subjected to multi-physical pre loads", *Smart Struct. Syst., Int. J.*, **23**(5), 429-447. https://doi.org/10.12989/sss.2019.23.5.429

Arefi, M. (2015), "The effect of different functionalities of FGM and FGPM layers on free vibration analysis of the FG circular plates integrated with piezoelectric layers", *Smart Struct. Syst., Int. J.*, **15**(5), 1345-1362. https://doi.org/10.12989/sss.2015.15.5.1345

Avcar, M. and Mohammed, W.K.M. (2018), "Free vibration of functionally graded beams resting on Winkler-Pasternak foundation", *Arab. J. Geosci.*, **11**(10), 232. https://doi.org/10.1007/s12517-018-3579-2

Baferani, A.H. and Saidi, A.R. (2013), "Effects of in-plane loads on vibration of laminated thick rectangular plates resting on elastic foundation: An exact analytical approach", *Eur. J. Mech.-A/Solids*, **42**, 299-314. https://doi.org/10.1016/j.euromechsol.2013.07.001

Beldjelili, Y., Tounsi, A. and Mahmoud, S.R. (2016), "Hygro-thermo-mechanical bending of S-FGM plates resting on variable elastic foundations using a four-variable trigonometric plate theory", *Smart Struct. Syst., Int. J.*, **18**(4), 755-786. https://doi.org/10.12989/sss.2016.18.4.755

Belmahi, S., Zidour, M., Meradjah, M., Bensattalah, T. and Dihaj, A. (2018), "Analysis of boundary conditions effects on vibration of nanobeam in a polymeric matrix", *Struct. Eng. Mech., Int. J.*, **67**(5), 517-525. https://doi.org/10.12989/sem.2018.67.5.517

Belmahi, S., Zidour, M. and Meradjah, M. (2019), "Small-scale effect on the forced vibration of a nano beam embedded an elastic medium using nonlocal elasticity theory", *Adv. Aircr. Spacecr. Sci., Int. J.*, **6**(1), 1-18. https://doi.org/10.12989/aas.2019.6.1.001

Benahmed, A., Houari, M.S.A., Benyoucef, S., Belakhdar, K. and Tounsi, A. (2017), "A novel quasi-3D hyperbolic shear deformation theory for functionally graded thick rectangular plates on elastic foundation", *Geomech. Eng., Int. J.*, **12**(1), 9-34. https://doi.org/10.12989/gae.2017.12.1.009

Benahmed, A., Fahsi, B., Benzair, A., Zidour, M., Bourada, F. and Tounsi, A. (2019), "Critical buckling of functionally graded nanoscale beam with porosities using nonlocal higher-order shear deformation", *Struct. Eng. Mech., Int. J.*, **69**(4), 457-466. https://doi.org/10.12989/sem.2019.69.4.457

Bensattalah, T., Bouakkaz, K., Zidour, M. and Hassaine Daouadji, T. (2018a), "Critical buckling loads of carbon nanotube embedded in Kerr's medium", *Adv. Nano Res., Int. J.*, **6**(4), 339-356. https://doi.org/10.12989/anr.2018.6.4.339

Bensattalah, T., Zidour, M. and Hassaine Daouadji, T. (2018b), "Analytical analysis for the forced vibration of CNT surrounding elastic medium including thermal effect using nonlocal Euler-Bernoulli theory", *Adv. Mater. Res., Int. J.*, **7**(3), 163-174. https://doi.org/10.12989/amr.2018.7.3.163

Bensattalah, T., Zidour, M., Hassaine Daouadji, T. and Bouakaz, K. (2019a), "Theoretical analysis of chirality and scale effects on critical buckling load of zigzag triple walled carbon nanotubes under axial compression embedded in polymeric matrix", *Struct. Eng. Mech., Int. J.*, **70**(3), 269-277. https://doi.org/10.12989/sem.2019.70.3.269

Bensattalah, T., Zidour, M. and Hassaine Daouadji, T. (2019b), "A new nonlocal beam model for free vibration analysis of chiral single-walled carbon nanotubes", *Compos. Mater. Eng., Int. J.*, **1**(1), 21-31. https://doi.org/10.12989/cme.2019.1.1.021

Bensattalah, T., Hassaine Daouadji, T. and Zidour, M. (2019c), "Influences the Shape of the Floor on the Behavior of Buildings Under Seismic Effect", *Proceedings of the 4th International Symposium on Materials and Sustainable Development*, Benmounah A., Abadlia M.T., Saidi M., Zerizer A. (eds), Springer, Cham, pp. 26-42. https://doi.org/10.1007/978-3-030-43268-3_3

Bouazza, M., Amara, K., Zidour, M., Tounsi, A. and Adda-Bedia, E.A. (2014a), "Hygrothermal effects on the postbuckling response of composite beams", *Am. J. Mater. Res.*, **1**(2), 35-43.

Bouazza, M., Amara, K., Zidour, M., Tounsi, A. and El Addas, A.B. (2014b), "Thermal effect on buckling of multiwalled carbon nanotubes using different gradient elasticity theories", *Nanosci. Nanotechnol.*, **4**(2), 27-33.

Bouazza, M., Amara, K., Zidour, M., Tounsi, A. and Adda-Bedia, E.A. (2015), "Postbuckling analysis of functionally graded beams using hyperbolic shear deformation theory", *Rev. Inform. Eng. Applicat.*, **2**(1), 1-14. https://doi.org/10.18488/journal.79/2015.2.1/79.1.1.14

Boulal, A., Bensattalah, T., Karas, A., Zidour, M., Heireche, H. and Bedia, E.A. (2020), "Buckling of carbon nanotube reinforced composite plates supported by Kerr foundation using Hamilton's energy principle", *Struct. Eng. Mech., Int. J.*, **73**(2), 209-223. https://doi.org/10.12989/sem.2020.73.2.209

Chen, Y.Z. (2018), "Transfer matrix method for solution of FGMs thick-walled cylinder with arbitrary inhomogeneous elastic response", *Smart Struct. Syst., Int. J.*, **21**(4), 469-477. https://doi.org/10.12989/sss.2018.21.4.469

Dihaj, A., Zidour, M., Meradjah, M., Rakrak, K., Heireche, H. and Chemi, A. (2018), "Free vibration analysis of chiral double-walled carbon nanotube embedded in an elastic medium using non-local elasticity theory and Euler Bernoulli beam model",

Struct. Eng. Mech., *Int. J.*, **65**(3), 335-342. https://doi.org/10.12989/sem.2018.65.3.335

Dorduncu, M. (2019), "Flexure Analysis of Functionally Graded Plates Using {2, 2}-Refined Zigzag Theory", *J. Aeronaut. Space Technol.*, **12**(1), 19-30.

Ebrahimi, F. and Barati, M.R. (2016), "A nonlocal higher-order shear deformation beam theory for vibration analysis of size-dependent functionally graded nanobeams", *Arab. J. Sci. Eng.*, **41**(5), 1679-1690. https://doi.org/10.1007/s13369-015-1930-4

Ebrahimi, F. and Daman, M. (2017), "Nonlocal thermo-electromechanical vibration analysis of smart curved FG piezoelectric Timoshenko nanobeam", *Smart Struct. Syst.*, *Int. J.*, **20**(3), 351-368. https://doi.org/10.12989/sss.2017.20.3.351

Fekrar, A., Houari, M.S.A., Tounsi, A. and Mahmoud, S.R. (2014), "A new five-unknown refined theory based on neutral surface position for bending analysis of exponential graded plates", *Meccanica*, **49**(4), 795-810. https://doi.org/10.1007/s11012-013-9827-3

Gafour, Y., Hamidi, A., Benahmed, A., Zidour, M. and Bensattalah, T. (2020), "Porosity-dependent free vibration analysis of FG nanobeam using non-local shear deformation and energy principle", *Adv. Nano Res.*, *Int. J.*, **8**(1), 37-47. https://doi.org/10.12989/anr.2020.8.1.037

Ghazzawi, S.M. and Abdelrahman, W.G. (2020), "Static Analysis of Thick Functionally Graded Plates with Different Property Distribution Functions", *Arab. J. Sci. Eng.*, **45**, 5099-5108. https://doi.org/10.1007/s13369-020-04344-6

Guessas, H., Zidour, M., Meradjah, M. and Tounsi, A. (2018), "The critical buckling load of reinforced nanocomposite porous plates", *Struct. Eng. Mech.*, *Int. J.*, **67**(2), 115-123. https://doi.org/10.12989/sem.2018.67.2.115

Hamidi, A., Zidour, M., Bouakkaz, K. and Bensattalah, T. (2018), "Thermal and small-scale effects on vibration of embedded armchair single-walled carbon nanotubes", *J. Nano Res.*, **51**, 24-38. https://doi.org/10.4028/www.scientific.net/JNanoR.51.24

Hirwani, C.K. and Panda, S.K. (2019), "Nonlinear finite element solutions of thermoelastic deflection and stress responses of internally damaged curved panel structure", *Appl. Mathe. Modell.*, **65**, 303-317. https://doi.org/10.1016/j.apm.2018.08.014

Hirwani, C.K., Panda, S.K., Mahapatra, T.R. and Mahapatra, S.S. (2017), "Numerical study and experimental validation of dynamic characteristics of delaminated composite flat and curved shallow shell structure", *J. Aerosp. Eng.*, **30**(5), 04017045. https://doi.org/10.1061/(ASCE)AS.1943-5525.0000756

Hirwani, C.K., Panda, S.K. and Mahapatra, T.R. (2018a), "Thermomechanical deflection and stress responses of delaminated shallow shell structure using higher-order theories", *Compos. Struct.*, **184**, 135-145. https://doi.org/10.1016/j.compstruct.2017.09.071

Hirwani, C.K., Panda, S.K. and Patle, B.K. (2018b), "Theoretical and experimental validation of nonlinear deflection and stress responses of an internally debonded layer structure using different higher-order theories", *Acta Mechanica*, **229**(8), 3453-3473. https://doi.org/10.1007/s00707-018-2173-8

Kar, V.R. and Panda, S.K. (2015), "Thermoelastic analysis of functionally graded doubly curved shell panels using nonlinear finite element method", *Compos. Struct.*, **129**, 202-212. https://doi.org/10.1016/j.compstruct.2015.04.006

Kar, V.R. and Panda, S.K. (2016), "Nonlinear thermomechanical behavior of functionally graded material cylindrical / hyperbolic /elliptical shell panel with dependent and ndependent temperature properties", *J. Press. Vessel Technol.*, **138**(6). https://doi.org/10.1115/1.4033701

Kar, V.R., Mahapatra, T.R. and Panda, S.K. (2015), "Nonlinear flexural analysis of laminated composite flat panel under hygro-thermo-mechanical loading", *Steel Compos. Struct.*, *Int. J.*, **19**(4), 1011-1033. https://doi.org/10.12989/scs.2015.19.4.1011

Katariya, P.V., Hirwani, C.K. and Panda, S.K. (2019), "Geometrically nonlinear deflection and stress analysis of skew sandwich shell panel using higher-order theory", *Eng. Comput.*, **35**(2), 467-485. https://doi.org/10.1007/s00366-018-0609-3

Khiloun, M., Bousahla, A.A., Kaci, A., Bessaim, A., Tounsi, A. and Mahmoud, S.R. (2019), "Analytical modeling of bending and vibration of thick advanced composite plates using a four-variable quasi 3D HSDT", *Eng. Comput.*, 1-15. https://doi.org/10.1007/s00366-019-00732-1

Lee, W.H., Han, S.C. and Park, W.T. (2015), "A refined higher order shear and normal deformation theory for E-, P-, and S-FGM plates on Pasternak elastic foundation", *Compos. Struct.*, **122**, 330-342. https://doi.org/10.1016/j.compstruct.2014.11.047

Mantari, J.L. and Soares, C.G. (2013), "A novel higher-order shear deformation theory with stretching effect for functionally graded plates", *Compos. Part B: Eng.*, **45**(1), 268-281. https://doi.org/10.1016/j.compositesb.2012.05.036

Neves, A.M.A., Ferreira, A.J.M., Carrera, E., Roque, C.M.C., Cinefra, M., Jorge, R.M.N. and Soares, C.M.M. (2012), "A quasi-3D sinusoidal shear deformation theory for the static and free vibration analysis of functionally graded plates", *Compos. Part B: Eng.*, **43**(2), 711-725. https://doi.org/10.1016/j.compositesb.2011.08.009

Nguyen, T.K. (2015), "A higher-order hyperbolic shear deformation plate model for analysis of functionally graded materials", *Int. J. Mech. Mater. Des.*, **11**(2), 203-219. https://doi.org/10.1007/s10999-014-9260-3

Nguyen, H.N., Hong, T.T., Vinh, P.V., Quang, N.D. and Thom, D.V. (2019), "A refined simple first-order shear deformation theory for static bending and free vibration analysis of advanced composite plates", *Materials*, **12**(15), 2385. https://doi.org/10.3390/ma12152385

Panda, K.B. and Chandran, K.R. (2003), "Titanium-titanium boride (Ti-TiB) functionally graded materials through reaction sintering: Synthesis, microstructure, and properties", *Metallurg. Mater. Transact. A*, **34**(9), 1993-2003. https://doi.org/10.1007/s11661-003-0164-3

Panda, S.K. and Singh, B.N. (2013), "Thermal Postbuckling Behavior of Laminated Composite Spherical Shell Panel Using NFEM#", *Mech. Based Des. Struct. Mach.*, **41**(4), 468-488. https://doi.org/10.1080/15397734.2013.797330

Radwan, A.F. and Zenkour, A.M. (2018), "Quasi 3-D trigonometric plate theory for bending analysis of EG plates resting on Pasternak foundations", *Curv. Layer. Struct.*, **5**(1), 146-155. https://doi.org/10.1515/cls-2018-0011

Shahsavari, D., Shahsavari, M., Li, L. and Karami, B. (2018), "A novel quasi-3D hyperbolic theory for free vibration of FG plates with porosities resting on Winkler/Pasternak/Kerr foundation", *Aerosp. Sci. Technol.*, **72**, 134-149 https://doi.org/10.1016/j.ast.2017.11.004

Shokravi, M. (2017), "Vibration analysis of silica nanoparticles-reinforced concrete beams considering agglomeration effects", *Comput. Concrete*, *Int. J.*, **19**(3), 333-338. https://doi.org/10.12989/cac.2017.19.3.333

Tayeb, T.S., Zidour, M., Bensattalah, T., Heireche, H., Benahmed, A. and Bedia, E.A. (2020), "Mechanical buckling of FG-CNTs reinforced composite plate with parabolic distribution using Hamilton's energy principle", *Adv. Nano Res.*, *Int. J.*, **8**(2), 135-148. https://doi.org/10.12989/anr.2020.8.2.135

Thai, H.T. and Kim, S.E. (2013), "A simple quasi-3D sinusoidal shear deformation theory for functionally graded plates", *Compos. Struct.*, *Int. J.*, **99**, 172-180. https://doi.org/10.1016/j.compstruct.2012.11.030

Vel, S.S. and Batra, R.C. (2003), "Exact thermoelasticity solution for cylindrical bending deformations of functionally graded

plates", In: *IUTAM Symposium on Dynamics of Advanced Materials and Smart Structures*, Watanabe K., Ziegler F. (eds), pp. 429-438. https://doi.org/10.1007/978-94-017-0371-0_42

Wu, C.P. and Liu, W.L. (2014), "3D buckling analysis of FGM sandwich plates under bi-axial compressive loads", *Smart Struct. Syst., Int. J.*, **13**(1), 111-135. https://doi.org/10.12989/sss.2014.13.1.111

Yi, S.C., Yao, L.Q. and Tang, B.J. (2017), "A novel higher-order shear and normal deformable plate theory for the static, free vibration and buckling analysis of functionally graded plates", *Mathe. Problems Eng.*, Article ID 6879508, 20 p. https://doi.org/10.1155/2017/6879508

Zenkour, A.M. (2009), "The refined sinusoidal theory for FGM plates on elastic foundations", *Int. J. Mech. Sci.*, **51**(11-12), 869-880. https://doi.org/10.1016/j.ijmecsci.2009.09.026

Zenkour, A.M. and Alghanmi, R.A. (2018), "Bending of functionally graded plates via a refined quasi-3D shear and normal deformation theory", *Curv. Layer. Struct.*, **5**(1), 190-200. https://doi.org/10.1515/cls-2018-0014

Zenkour, A.M. and Radwan, A.F. (2018), "Compressive study of functionally graded plates resting on Winkler–Pasternak foundations under various boundary conditions using hyperbolic shear deformation theory", *Arch. Civil Mech. Eng.*, **18**(2), 645-658. https://doi.org/10.1016/j.acme.2017.10.003

Zerrouki, R., Karas, A. and Zidour, M. (2020), "Critical buckling analyses of nonlinear FG-CNT reinforced nano-composite beam", *Adv. Nano Res., Int. J.*, **9**(3), 211-220. https://doi.org/10.12989/anr.2020.9.3.211

CC